# Co-optimisation of Planning and Operation for Active Distribution Grids

Stavros Karagiannopoulos*, Petros Aristidou†, Gabriela Hug*
* EEH - Power Systems Laboratory, ETH Zurich, Physikstrasse 3, 8092 Zurich, Switzerland
† School of Electronic and Electrical Engineering, University of Leeds, Leeds LS2 9JT, UK
Emails: {karagiannopoulos, hug}@eeh.ee.ethz.ch, p.aristidou@leeds.ac.uk

***Abstract*—Given the increased penetration of smart grid technologies, distribution system operators are obliged to consider in their planning stage both the increased uncertainty introduced by non-dispatchable distributed energy resources, as well as the operational flexibility provided by new real-time control schemes. First, in this paper, a planning procedure is proposed which considers both traditional expansion measures, e.g. upgrade of transformers, cables, etc., as well as real-time schemes, such as active and reactive power control of distributed generators, use of battery energy storage systems and flexible loads. At the core of the proposed decision making process lies a tractable iterative AC optimal power flow method. Second, to avoid the need for a real-time centralised coordination scheme (and the associated communication requirements), a local control scheme for the operation of individual distributed energy resources and flexible loads is extracted from offline optimal power flow computations. The performance of the two methods is demonstrated on a radial, low-voltage grid, and compared to a standard local control scheme.**

***Index Terms*—AC optimal power flow, distribution grid planning, distribution grid operation**

## I. Introduction

Distribution grids are facing significant changes due to the introduction of Distributed Energy Resources (DERs) in medium and Low Voltage (LV) levels. Electric vehicles, PhotoVoltaic (PV) units, Battery Energy Storage Systems (BESS), flexible loads and other DERs bring not only new opportunities, but also challenges to the Distribution System Operators (DSOs). On the one hand, the increasing level of DER installations can create several technical problems to the DSOs, many of which are already visible in modern day distribution grids. On the other hand, the DSOs can now use the DERs to increase the observability and controllability of their grid and provide ancillary services to the network. However, to exploit these new resources available to them, more sophisticated tools and methods are needed in the planning and operation stages.

The transition towards active distribution grids, i.e. considering also the control possibilities of DERs, is recognised as a necessity for modern DSOs. Reference [1] discusses in detail planning, optimisation and reliability aspects of future grids and describes the evolution from a passive system based on a fit-and-forget approach to active management of the grid. For such a transformation, the traditional grid planning methods are inefficient, since they usually neglect the active participation of DERs [2].

The question of how to optimally plan distribution systems in a traditional setting without the consideration of active control capabilities has been addressed in many publications [3]–[8]. Most approaches are based on optimisation formulations, e.g. mixed integer linear/nonlinear problems MILP [3], MINLP [4], while others use metaheuristic algorithms, such as the Genetic Algorithm [5]. A detailed review on models and methods of distribution system planning is presented in [8], where the interested reader can find extensive information in terms of commonly used objective functions, measures considered, as well as which parts of distribution networks are optimised. Most of the reviewed papers focus on the feeder and substation location (routing) and size.

The consideration of operational aspects into the planning problem has only recently been examined [9], [10]. The authors of [9] use a tractable iterative multi-period AC Optimal Power Flow (AC OPF) problem to investigate in which BESS price ranges distributed or centralized storage would be more meaningful in LV grids. The BESS are operated by residential customers having access to energy markets and trying to maximise their self-consumption. In [10], a planning methodology using the non-linear single-period AC OPF formulation is presented, where the optimal decisions are based on either purely conventional upgrade measures or on controlling active and reactive power of modern units. Most of these publications assume perfect communication between a centralized controller and the controlled units.

The contribution of this paper is twofold. First, we present a decision-making tool which co-optimizes investment and operational decisions in distribution grids. As investment decisions, we consider the installation of grid upgrade measures including new branches (cables or transformers) and BESS. The considered active measures include Active Power Curtailment (APC), Reactive Power Control (RPC) and Controllable Loads (CL). These fall into the category of investment deferral measures, all of which incur operational cost to the DSO. An iterative AC OPF formulation, based on the backward-forward sweep technique [9], is adapted and extended to consider both conventional upgrade options and active measures, transforming the problem into a MILP. This formulation captures combinations of traditional grid expansion measures with control of DERs, and includes the inter-temporal constraints of BESS and CLs. In this work, we assume that there is no regulatory framework imposing a certain planning procedure to the DSOs. That way, in case the security of supply is not

endangered, a DSO can choose freely among conventional grid expansion methods, active measures, or a combination of both. This is currently the case in microgrids.

The second contribution relates to the real-time operation of the grid when centralised control capabilities and extended communication infrastructure are not available. This paper extends the method in [11] of extracting local DER control schemes, to include CLs and their time-coupling constraints. These local control schemes ideally yield the same (or similar) results as that of a centralized control scheme. The extraction method is based on running the centralised problem off-line and obtaining the optimal set-points for the DERs; then, the individual characteristic curves for each DER are derived from these results for use in the operation stage. This scheme uses only local measurements to address system-wide issues and tries to mimic the OPF response without the need for communication.

The remainder of the paper is organized as follows: in Sections II and III, the mathematical formulation of the joint planning and operation stages is presented. Section IV describes the considered case study and the simulation results. Finally, conclusions are drawn in Section V.

## II. Joint planning and operation stages

In this section, we will derive and justify the MILP formulation lying at the core of the proposed decision process. The objective of the DSO is to minimize the sum of the planning and operating costs. The costs of all available planning options are converted to an Equivalent Annual Cost (EAC), to account for their different lifetimes. This conversion is given as:

$$EAC = \frac{\text{Asset Price} \cdot \text{Discount Rate}}{1-(1+\text{Discount Rate})^{\text{-Number of periods}}} \tag{1}$$

Thus, the objective function corresponds to

$$\min_{\text{u, Z}} \left(c^{\text{T}}_{\text{inv}} \cdot Z + c^{\text{T}}_{\text{op}} \cdot u\right) \tag{2}$$

where vector $c^{\text{T}}_{\text{inv}}$ represents the EAC of the investment costs associated with the installation of new hardware (linked with binary $Z$), and vector $c^{\text{T}}_{\text{op}}$ the operational costs associated with the activated control measures' vector $u$ which includes the dispatch of the active/reactive outputs of DERs, the activation of flexible loads, the modification of BESS setpoints, etc.

More specifically, the DSO optimizes the vector $\mathcal{X} = [P^{\text{f}}_{\text{g}}, P^{\text{f}}_{\text{l,flex}}, E^{\text{bat}}_{\text{inv}}, P^{\text{ch}}_{\text{B}}, P^{\text{dis}}_{\text{B}}, Q^{\text{f}}_{\text{f}}, Z, V_{\text{f}}]$ over the objective function

$$\begin{aligned}\min_{\mathcal{X}} \sum_{\text{i=1}}^{N_{\text{l}}} c^{\text{b}}_{\text{inv}} \cdot Z_{\text{i}} + \sum_{\text{j=1}}^{N_{\text{b}}} c^{\text{bat}}_{\text{inv}} \cdot E^{\text{bat}}_{\text{inv,j}} + \\ + \sum_{j=1}^{N_{\text{b}}} \sum_{t=1}^{N_{\text{hor}}} (c^{\text{T}}_{\text{P}} \cdot P_{\text{curt,j,t}} + c^{\text{T}}_{\text{Q}} \cdot Q_{\text{ctrl,j,t}}) \cdot \Delta t\end{aligned} \tag{3}$$

where $E^{\text{bat}}_{\text{inv,j}}$ is the BESS capacity to be installed at node $j$, with $N_{\text{b}}$ being the total number of nodes; $Z_{\text{i}}$ is a binary decision variable corresponding to the investment of a new cable or transformer at branch $i$, and $N_{\text{l}}$ is the number of branches; $P_{\text{curt,j,t}} = P_{\text{max,j,t}} - P^{\text{f}}_{\text{g,j,t}}$ is the curtailed power of the DER unit at node $j$ and time $t$, $P_{\text{max,j,t}}$ the maximum active power it can inject at this time, $P^{\text{f}}_{\text{g,j,t}}$ its actual infeed, and $N_{\text{hor}}$ the time horizon studied. The use of the reactive power $Q^{\text{f}}_{\text{g,j,t}}$ for each DER at node $j$ and time $t$ is minimized by including the term $Q_{\text{ctrl,j,t}} = |Q^{\text{f}}_{\text{g,j,t}}|$ in the objective function. Finally, $c^{\text{b}}_{\text{inv}}$ represents the cost of investing in a new branch element, $c^{\text{T}}_{\text{P}}$ the cost of curtailing active power, and $c^{\text{T}}_{\text{Q}}$ the cost of using reactive power. Although $c^{\text{T}}_{\text{P}}$ is an actual cost which depends on the regulation of each area, $c^{\text{T}}_{\text{Q}}$ is an artificial cost to avoid extensive use of RPC, representing a penalty on control effort. Selecting $c^{\text{T}}_{\text{Q}} \ll c^{\text{T}}_{\text{P}}$ allows prioritizing the use of reactive power control over active power curtailment.

The OPF formulation also needs to include all pertinent constraints. This includes the power balance equations at every node $j = [1, ..., N_b]$ and time step $t$ as given by

$$P^{\text{f}}_{\text{inj,j,t}} = P^{\text{f}}_{\text{g,j,t}} - P^{\text{f}}_{\text{lflex,j,t}} - (P^{\text{ch}}_{\text{B,j,t}} - P^{\text{dis}}_{\text{B,j,t}}) \tag{4}$$

$$Q^{\text{f}}_{\text{inj,j,t}} = Q^{\text{f}}_{\text{g,j,t}} - P^{\text{f}}_{\text{lflex,j,t}} \cdot tan(\arccos(pf)) \tag{5}$$

where for each node $j$ and time step $t$, $P^{\text{f}}_{\text{g,j,t}}$ and $Q^{\text{f}}_{\text{g,j,t}}$ are the active and reactive power infeeds of the DERs; $P^{\text{f}}_{\text{lflex,j,t}}$ and $P^{\text{f}}_{\text{lflex,j,t}} \cdot tan(\arccos(pf))$ are the final active and reactive node demand, with $pf$ being the power factor of the load; $P^{\text{ch}}_{\text{B,j,t}}$ and $P^{\text{dis}}_{\text{B,j,t}}$ are respectively the charging and discharging power of the BESS; $P^{\text{f}}_{\text{inj,j,t}}$ and $Q^{\text{f}}_{\text{inj,j,t}}$ are the net active and reactive power injections of the nodes;

In the used MILP representation, the power balance equations are incorporated in the following form

$$P^{\text{f}}_{\text{inj,j,t}} = M_{\text{l}} \cdot P_{\text{line,i,t}} \quad Q^{\text{f}}_{\text{inj,j,t}} = M_{\text{l}} \cdot Q_{\text{line,i,t}} \tag{6}$$

where $M_{\text{l}}$ is a mapping matrix needed for the Power Flow (PF) calculations [12]; and, $P_{\text{line,i,t}}$ and $Q_{\text{line,i,t}}$ are the active and reactive power flows of each branch $i$ and time step $t$. It has to be noted that in this work an active DSO is assumed to have control over the DER setpoints, the BESS charging and discharging behaviour, and the flexible load response, i.e. the owners of the components follow the instructions of the DSO. The voltage constraints at nodes $j$=$[2, ..., N_{\text{b}}]$ are given by

$$V_{\text{min}} \leq |V_{\text{j,t}}| \leq V_{\text{max}} \tag{7}$$

where $V_{\text{max}}$, $V_{\text{min}}$ are the upper and lower acceptable voltage magnitude limits. The voltage magnitude and angle at the substation are fixed and equal to $|V_1| = 1\text{p.u.}$, $\theta_1 = 0°$. The following approximation is used for the MILP representation:

$$|\Delta V_{\text{j,t}}| \approx Re\left\{B_{\text{V}} \cdot (P^{\text{f}}_{\text{inj,j,t}} + jQ^{\text{f}}_{\text{inj,j,t}})^*\right\} \tag{8}$$

$$|V_{\text{j,t}}| = |V_1| + |\Delta V_{\text{j,t}}| \tag{9}$$

where $B_{\text{V}}$ captures the grid structure and the impedance information, and is required for the iterative PF calculations [9], in order to approximate the voltage drops in LV grids. Similarly, the thermal limits of the distribution lines are imposed by

$$(P_{\text{line,i,t}})^2 + (Q_{\text{line,i,t}})^2 \leq (S^{\text{max}}_{\text{i}})^2 + sl_{\text{i}} \tag{10}$$

In the MILP representation we substitute (10) with

$$P_{\text{line,i,t}} \leq (S_{\text{i}}^{\max} + sl_{\text{i}}) \pm \frac{1-\cos\varphi_2}{\sin\varphi_2} \cdot Q_{\text{line,i,t}} \quad (11)$$

$$P_{\text{line,i,t}} \geq -(S_{\text{i}}^{\max} + sl_{\text{i}}) \pm \frac{1-\cos\varphi_2}{\sin\varphi_2} \cdot Q_{\text{line,i,t}} \quad (12)$$

$$Q_{\text{line,i,t}} \leq (S_{\text{i}}^{\max} + sl_{\text{i}}) \cdot \sin\varphi_2 \quad (13)$$

$$Q_{\text{line,i,t}} \geq -(S_{\text{i}}^{\max} + sl_{\text{i}}) \cdot \sin\varphi_2 \quad (14)$$

$$0 \leq sl_{\text{i}} \leq 100 \cdot Z_{\text{i}} \quad (15)$$

where $S_{\text{i}}^{\max}$ is the apparent power corresponding to the upper thermal limit of branch $i$, $sl_{\text{i}}$ a slack variable linked with the binary $Z_{\text{i}}$ to indicate that additional capacity is needed at branch $i$, and $\varphi_2$ is the angle that approximates the quadratic constraint with linear constraints following [12]. The DER limits are given by

$$P_{\text{g,j}}^{\min} \leq P_{\text{g,j,t}}^{\text{f}} \leq P_{\text{g,j}}^{\max}, \qquad Q_{\text{g,j}}^{\min} \leq Q_{\text{g,j,t}}^{\text{f}} \leq Q_{\text{g,j}}^{\max} \quad (16)$$

$$-\tan(\phi_{\max}) P_{\text{g,j,t}}^{\text{f}} \leq Q_{\text{g,j,t}}^{\text{f}} \leq \tan(\phi_{\max}) P_{\text{g,j,t}}^{\text{f}} \quad (17)$$

where $P_{\text{g,j}}^{\min}$, $P_{\text{g,j}}^{\max}$, $Q_{\text{g,j}}^{\min}$, $Q_{\text{g,j}}^{\max}$ are the upper and lower limits for active and reactive DER generation at each node $j$. These limits vary depending on the type of the DER and the control schemes implemented. Usually, small inverter-based generators have technical or regulatory [13] limitations on the power factor they can operate at. Here, the reactive power limit is modified to (17), where $cos(\tan(\phi_{\max}))$ is the maximum power factor.

The behaviour of the flexible load at node $j$ is given by

$$P_{\text{lflex,j,t}} = P_{\text{l,j,t}} + x \cdot P_{\text{shift,j}} - y \cdot P_{\text{shift,j}}, \qquad x + y \leq 1 \quad (18)$$

$$\sum_{t=1}^{24} (P_{\text{lflex,j,t}} - P_{\text{l,j,t}}) = 0 \quad (19)$$

where $P_{\text{lflex,j,t}}$ is the final controlled active demand at node $j$ and time $t$, $P_{\text{shift,j}}$ being the shiftable load at node $j$, $x$ and $y$ being binary variables assuring that the load is either increased, or decreased when shifted. The final constraint assures that the final total daily energy demand is maintained. Although this formulation of flexible loads is rather general, it captures the main characteristics of inter-temporal coupling, and can be easily adjusted by DSOs in presence of more detailed models.

Finally, the constraints related to the BESS are given as

$$SoC_{\text{min}}^{\text{bat}} \cdot E_{\text{inv,j}}^{\text{bat}} \leq E_{\text{j,t}}^{\text{bat}} \leq SoC_{\text{max}}^{\text{bat}} \cdot E_{\text{inv,j}}^{\text{bat}} \quad (20)$$

$$E_{\text{j,1}}^{\text{bat}} = E_{\text{start}} \quad (21)$$

$$P_{\text{B,j,t}}^{\text{ch}} \geq 0, \qquad P_{\text{B,j,t}}^{\text{dis}} \geq 0 \quad (22)$$

$$P_{\text{B,j,t}}^{\text{ch}} \cdot P_{\text{B,j,t}}^{\text{dis}} \leq \epsilon \quad (23)$$

In order to avoid the bi-linearity, we use

$$P_{\text{B,j,t}}^{\text{ch}} \cdot (P_{\text{l,j,t}} - P_{\text{g,j,t}}^{\text{f}}) \leq \epsilon \quad (24)$$

$$P_{\text{B,j,t}}^{\text{dis}} \cdot (P_{\text{l,j,t}} - P_{\text{g,j,t}}^{\text{f}}) \geq \epsilon \quad (25)$$

$$E_{\text{j,t}}^{\text{bat}} = E_{\text{j,t-1}}^{\text{bat}} + (\eta_{\text{bat}} \cdot P_{\text{B,j,t}}^{\text{ch}} - \frac{P_{\text{B,j,t}}^{\text{dis}}}{\eta_{\text{bat}}}) \cdot \Delta t \quad (26)$$

where $E_{\text{inv,j}}^{\text{bat}}$ is the installed BESS capacity at node $j$, $E_{\text{j,t}}^{\text{bat}}$ is the available energy capacity at node $j$ and time $t$ assuming $E_{\text{start}}$ initial energy BESS content and constrained by $SoC_{\text{min}}^{\text{bat}}$, $SoC_{\text{max}}^{\text{bat}}$ which are the fixed minimum and maximum per unit limits; $P_{\text{B,j,t}}^{\text{ch}}$ and $P_{\text{B,j,t}}^{\text{dis}}$ are the charging and discharging BESS power, with (24)-(25) making sure that the BESS is not charging and discharging at the same time, by using an arbitrarily small value $\epsilon = 10^{-5}$; finally, (26) defines the energy capacity at each time step $t$ influenced by the BESS efficiency $\eta_{\text{bat}}$ and accounting for the time interval $\Delta t$.

## III. Real time operation Stage

Once the planning decisions are made, the DSO is responsible for the safe grid operation in real time. The methodology presented in Section II assumes distribution grids with perfect communication infrastructure, where all measurements are gathered at the DSO and a network-level optimization is used to compute the system-wide, optimal, DER setpoints. Thus, the corresponding real-time operation requires solving the MILP problem given by

$$\begin{aligned} &\min_{u} \ (c_{\text{op}}^{T} \cdot u) \\ &\text{s.t.} \qquad (4)-(14), \quad (16)-(26) \end{aligned} \quad (27)$$

However, in many occasions, the necessary communication infrastructure is not yet available. For this reason, a methodology was proposed in [11] to devise a decentralised control scheme to approximate the optimal behaviour using only local measurements. The characteristic curves $Q = f(V, P)$ and $P_{\text{curt}} = f(V, P)$ dictating the real-time behaviour of each inverter were extracted based on the offline solution of (27) and historical data, load, and generation forecasts.

In this work, Algorithm 1 extends the methods presented in [11] to derive local control schemes for the decentralised behaviour of flexible loads. It is assumed that part of the load ($P_{\text{shift}}$) can be shifted in time, but the total daily consumption has to remain constant. Once the local voltage exceeds some predefined lower (upper) threshold $V_{\text{thr}}^{\text{low}}$ ($V_{\text{thr}}^{\text{up}}$) and there is adequate time ahead to maintain the total daily demand constant, the load is decreased (increased). Later on, as the voltage lies between acceptable thresholds, the load is adjusted so that the final daily consumption is kept. This type of load is controlled in a discrete way, and can correspond to thermally activated buildings. A detailed building model or the impact of shifting on the total efficiency are outside of this paper's scope. For detailed models and analysis of ancillary services offered by buildings, the interested reader is referred to [14].

## IV. Case study

### A. Test System

We demonstrate the proposed methods using the benchmark radial LV grid presented in [15] and sketched in Fig. 1. Even though these networks may exhibit unbalanced operation, in this work we focus on the planning stage assuming balanced system loading. The parameters for the loads and the cables, are taken from [15]. The installed PV capacity is expressed as a percentage of the total load and is summarized here; DER nodes $= [12, 16, 18, 19]$, PV share $(\%) = [20, 60, 30, 30]$.

**Algorithm 1** Local control for loads $P_{lflex,t} = f(V, P_l, t)$

**Input:** $P_{\text{shift}}$, $P_{\text{l,t}}$, $V_{\text{thr}}^{\text{low}}$, $V_{\text{thr}}^{\text{up}}$
**Output:** $P_{\text{lflex,t}}$

**Initialize:** $\Delta P = 0$
**if** $(V_t < V_{\text{thr}}^{\text{low}}) \& (|\frac{\Delta P}{P_{\text{shift}}}| < 24 - t)$ **then**
  Reduce load: $P_{\text{lflex,t}} = P_{\text{l,t}} - P_{\text{shift}}$
  Update power mismatch: $\Delta P = \Delta P + P_{\text{shift}}$
**else if** $(V_{\text{thr}}^{\text{low}} \leq V_t \leq V_{\text{thr}}^{\text{up}})$ & $(\Delta P \neq 0)$ **then**
  **if** $\Delta P > 0$ **then**
    Increase load: $P_{\text{lflex,t}} = P_{\text{l,t}} + P_{\text{shift}}$
    Update power mismatch: $\Delta P = \Delta P - P_{\text{shift}}$
  **else**
    Reduce load: $P_{\text{lflex,t}} = P_{\text{l,t}} - P_{\text{shift}}$
    Update power mismatch: $\Delta P = \Delta P + P_{\text{shift}}$
  **end if**
**else if** $(V_t > V_{\text{thr}}^{\text{up}}) \& (|\frac{\Delta P}{P_{\text{shift}}}| < 24 - t)$ **then**
  Increase load: $P_{\text{lflex,t}} = P_{\text{l,t}} + P_{\text{shift}}$
  Update power mismatch: $\Delta P = \Delta P - P_{\text{shift}}$
**end if**
**return** $P_{\text{lflex,t}}$

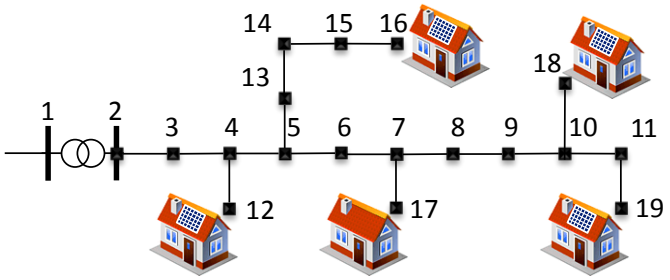


Fig. 1. Cigre LV grid - modified [15].

In order to capture the time variability, we use representative and worst-case days for the different seasons with different weights. We test the performance of our methods using 4 worst and 4 representative days, i.e. 2 days per season, therefore simulating the annual behavior by running a 192-hour multi-period OPF problem with a time resolution of 1 hour.

### *B. Case study - Cable Overload and Overvoltage*

In this case study, we investigate the planning options of a DSO being responsible for the above described grid with large PV integration that causes voltage and overload problems.

First, the network problems are identified by simulating the representative days. It can be seen in Fig. 2 that the voltage limits (set to 1.1p.u.) at Node 16 are exceeded. In addition, overloading of the cable connecting nodes $4-12$ is observed.

It has to be noted that the optimal planning decision which considers also operational aspects is case-dependent and varies from area to area. The driving factors which define the best DSO actions are the investment and operating costs. These can be very different even within the same country, depending on labor costs as well as on where the installation will take place, e.g. installing a cable in the center of a big city is much more expensive than in a rural area.

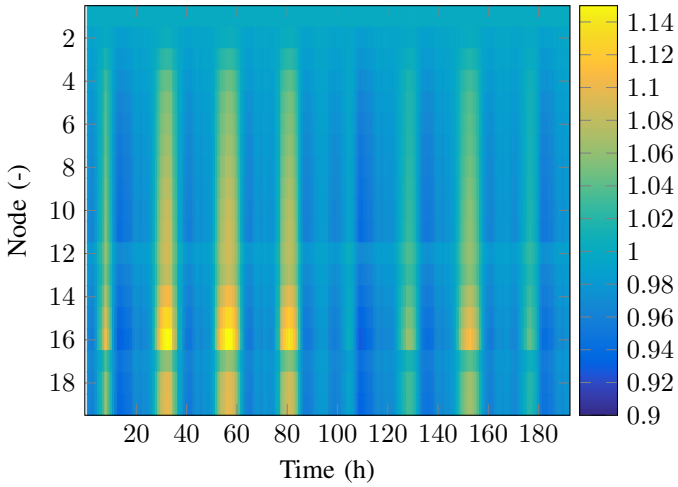


Fig. 2. Voltage magnitude for the worst and the typical days.

TABLE I
PLANNING OPTIONS FOR ACTIVE DSOS.

| Planning options : | Lifetime (y) | Projected cost evolution | Sensitivity analysis ranges |
|---|---|---|---|
| Cable (CHF/m) | 40 | $\approx$ | 50-150 |
| Transformer (CHF/kVA) | 20-40 | $\approx$ | 25 |
| BESS (CHF/kWh) | 5-10 | $\downarrow\downarrow\downarrow$ | 600-200 |
| APC (CHF/kWh) | - | $\downarrow\approx\uparrow$ | 0.1-0.4 |
| RPC (CHF/kWh) | - | $\approx 0$ | 1% $C_{APC}$ |
| CL (CHF/kWh) | - | $\downarrow\approx\uparrow$ | $\approx 0$ |

*1) Sensitivity Analysis:* In order to show the influence of the various costs on the optimal results, a sensitivity analysis is performed, varying the most important cost units. Table I shows the assumed lifetime, projected cost evolution and the final considered ranges of the different planning options. In this work, we assume that material costs for cables and transformers will remain the same, while the cost of BESS will decrease in the coming years. The operational costs of the examined control schemes are more difficult to derive since they depend more on regulation and policy rather than on material costs. In the future, the DSOs may be obliged to compensate PV owners based on some feed-in tariff for curtailing their active power or for providing reactive power control and other ancillary services. Assigning costs to shifting loads is even more complex due to the large variety of load types. For instance, shifting thermal loads with fixed daily needs might not lead to any additional costs.

Figure 3 shows the DSO EAC with the unit costs / prices varying according to Table I and using the methodology described in Section II. Thus, we can identify in which ranges, different planning options are most cost efficient. The numbers at the vertices show which percentage of the EAC is spent on each planning option. For both cases, low curtailment cost ($\leq 0.2\frac{\text{CHF}}{\text{kWh}}$) indicate APC as the most preferable option (used to 100%). As this cost increases, other measures are also utilized, e.g. BESS if they are cheap ($\leq 200\frac{\text{CHF}}{\text{kWh}}$) or an additional cable when $C_{\text{curt}} \geq 0.3\frac{\text{CHF}}{\text{kWh}}$, as depicted in Fig. 3(a) for which $C_{\text{cable}} = 50\frac{\text{CHF}}{\text{m}}$. For higher cable cost, APC and BESS are used almost in all cases, as seen in Fig. 3(b).

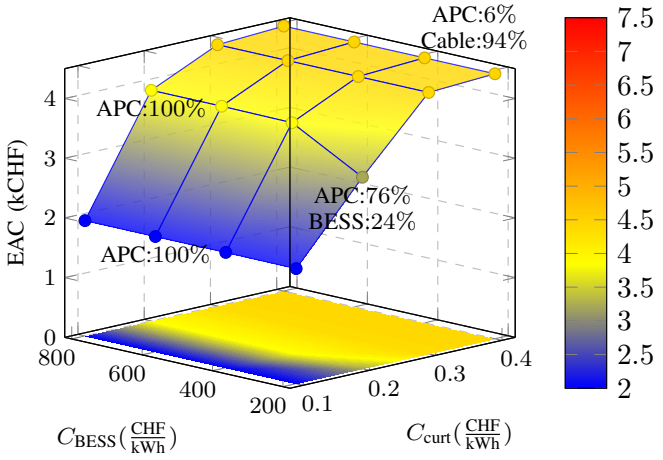


(a) $C_{\text{cable}} = 50(\frac{\text{CHF}}{\text{m}})$

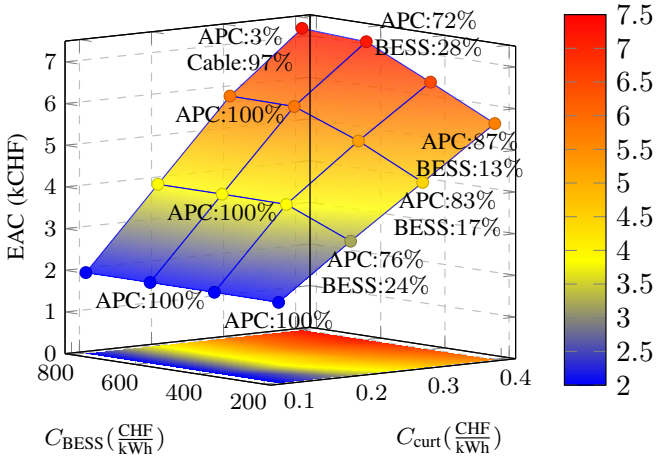


(b) $C_{\text{cable}} = 100(\frac{\text{CHF}}{\text{m}})$

Fig. 3. DSO equivalent annual cost for different costs.

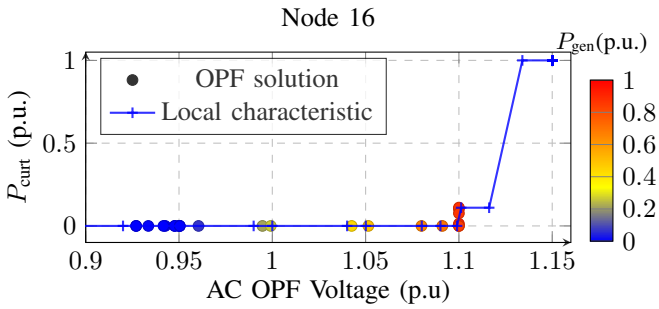


(a) $Q{=}f(V,P)$ characteristic curve at Node 16.

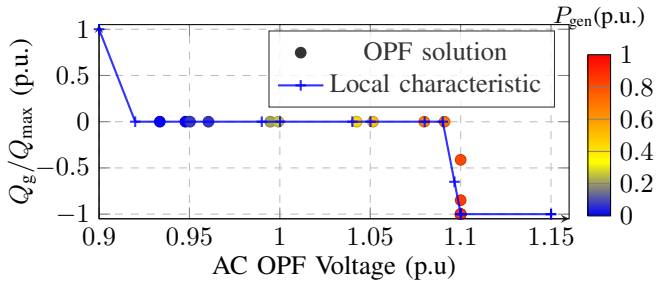


(b) $P_{curt}{=}f(V,P)$ characteristic curve at Node 16.

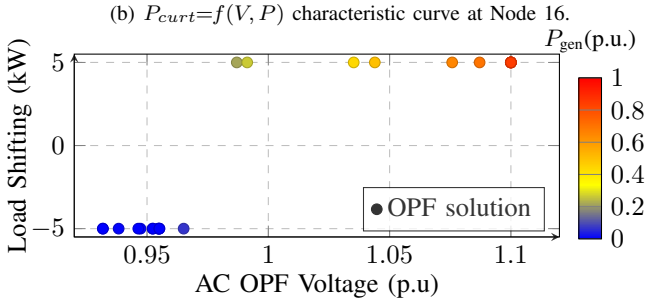


(c) Optimal load shifting at Node 16.

Fig. 4. Characteristic curves and optimal load shifting at Node 16.

### C. Operation Stage

Under the assumption of a fully controllable grid and a perfect communication infrastructure, the DSO would be able to continuously update the setpoints of all units by running OPF calculations with updated measurements of the PV and load injections. However, most of the current distribution grids do not have such advanced communication and control capabilities (yet). Thus, in this section we derive a decentralised control scheme (based only on local measurements) that closely approaches the OPF response. Following the methodology of [11], we use the optimal DER setpoints from the OPF-based control of (27), applied to the worst summer day to obtain the $Q = f(V, P)$ and $P_{\text{curt}} = f(V, P)$ characteristic curves for all nodes. Figures 4(a) and 4(b) show the corresponding curves for a PV unit and Fig. 4(c) shows the optimal shifting of a flexible load, all connected to Node 16.

Simulating the above system with different PV injection and load conditions can allow us to quantify the benefits of using the optimised decentralised control scheme over existing local schemes (as defined by current grid codes). Thus, we compare the performance of the following methods

- *No control*: This case corresponds to simple AC PF for each time step. The PVs are operated having a power factor of one (i.e., without reactive control);
- *OPF-based control*: A centralised approach is assumed here, where the DERs receive the optimal operational setpoints from the OPF solution.
- *Default local control*: In this case, the PVs behave according to the characteristic curve of the German grid-codes [13]. As soon as they inject more than half of their maximum power, they have to adjust their power factor.
- *Optimised local control*: Finally, in this case each inverter is equipped with different characteristic curves according to [11], and the flexible loads according to Algorithm 1 with $V_{\text{thr}}^{\text{low}} = 1.08$ p.u. and $V_{\text{thr}}^{\text{up}} = 0.94$ p.u., considering the 2 worst upper / lower optimal setpoints of Fig. 4(c).

In the following results, we simulate the grid behavior according to all methods for 30 summer days, i.e. the PV injection and load scaling factors are taken from June.

Figure 5 shows the evolution of the voltage at the problematic Node 16 over the whole month. It can be seen that having no control or operating with the current German regulation

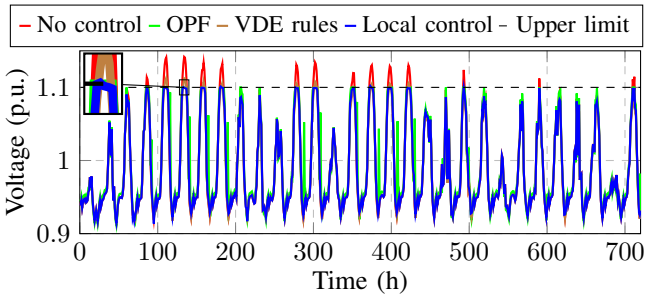


Fig. 5. Voltage evolution according to all methods at Node 16.

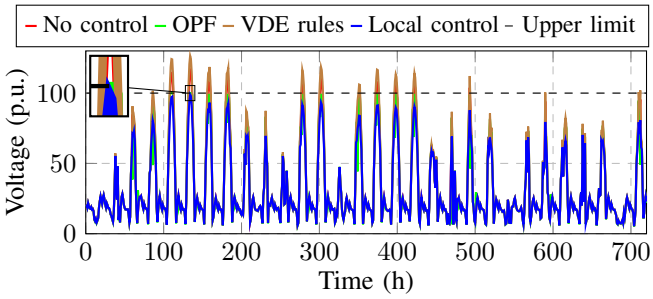


Fig. 6. Loading evolution at Cable 4-12.

leads to frequent voltage limit violations when the difference of PV injection and load is large. On the contrary, both the OPF-based and the optimised local control satisfy the voltage security constraints. Figure 6 shows the loading of the problematic cable 4–12 over the whole month. In this case, the current VDE rules show worse results than without any control due to the increased need for reactive power at Node 12. Both the OPF–based and the proposed local control satisfy the constraint. The first achieves this with the least possible cost, while the latter shows reduced maximum loading due to higher APC (and cost). Finally, Fig. 7 compares the load shifting of the OPF–based against the optimized local control over a period of 2 days. It can be seen that the first makes more frequent use of the flexibility offered by the load, as it is not triggered exclusively by the local voltage values. The optimized local control initiates load shifting mostly at noon hours in order to reduce the local voltage, and once the voltage is within acceptable limits, compensates for the earlier load increase.

## V. Conclusion

DSOs have nowadays a variety of tools in their disposal to face the planning and operational challenges of the future. These include both conventional expansion decisions as well as active measures. This paper presents a decision-making tool to assist DSOs decide on their planning and operation decisions. By co-optimizing the planning and the operation stages, DSOs can assess the trade-offs among the different alternatives and find the optimal balance between hardware-based grid extensions and active grid management. The decision process is formulated as a mixed integer linear problem (MILP), using a tractable iterative AC OPF problem. A sensitivity analysis was performed, varying the most important costs. It demonstrates that the optimal solution is case-dependent and there is no "one-size-fits-all" solution.

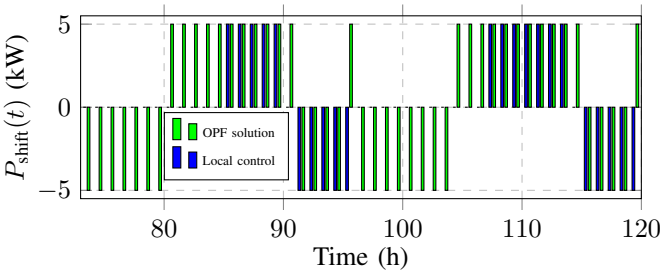


Fig. 7. Load shifting at Node 16.

Finally, in the transitional phase where extensive communication and control infrastructure is not available in real-time operation, an optimised local control scheme is also presented, tuned by off-line calculations, to provide a near-optimal behaviour for flexible loads. Results for a summer month show that it is slightly more conservative than the OPF-based control and does not lead to security constraint violations.

## References


[1] Working Group C6.19, "Planning and Optimization Methods for Active Distribution Systems Working Group C6.19," Cigre, Tech. Rep. Aug., 2014.

[2] Smart Planning Project WP 2.5, "Planning practices of electrical distribution grids."

[3] P. Paiva, H. Khodr, J. Dominguez-Navarro, J. Yusta, and A. Urdaneta, "Integral planning of primary-secondary distribution systems using mixed integer linear programming," *IEEE Transactions on Power Systems*, vol. 20, no. 2, pp. 1134–1143, 2005.

[4] S. Mohtashami, D. Pudjianto, and G. Strbac, "Strategic Distribution Network Planning With Smart Grid Technologies," *IEEE Transactions on Smart Grid*, vol. PP, no. 99, p. 1, 2016.

[5] E. Naderi, H. Seifi, and M. S. Sepasian, "A dynamic approach for distribution system planning considering distributed generation," *IEEE Transactions on Power Delivery*, vol. 27, no. 3, pp. 1313–1322, 2012.

[6] C. K. Gan, P. Mancarella, D. Pudjianto, and G. Strbac, "Statistical appraisal of economic design strategies of LV distribution networks," *Electric Power Systems Research*, vol. 81, no. 7, pp. 1363–1372, 2011.

[7] F. Pilo, G. Celli, E. Ghiani, and G. Soma, "New electricity distribution network planning approaches for integrating renewable," *Wiley Interdisciplinary Reviews: Energy and Environment*, vol. 2, no. 2, pp. 140–157, 3 2013.

[8] P. S. Georgilakis and N. D. Hatziargyriou, "A review of power distribution planning in the modern power systems era: Models, methods and future research," *Electric Power Systems Research*, vol. 121, pp. 89–100, 2015.

[9] P. Fortenbacher, M. Zellner, and G. Andersson, "Optimal Sizing and Placement of Distributed Storage in Low Voltage Networks," in *19th Power Systems Computation Conference 2016*, Genoa, Italy, 2016.

[10] S. Karagiannopoulos, P. Aristidou, A. Ulbig, S. Koch, and G. Hug, "Optimal planning of distribution grids considering active power curtailment and reactive power control," *IEEE Power and Energy Society General Meeting*, 2016.

[11] S. Karagiannopoulos, P. Aristidou, and G. Hug, "Hybrid approach for planning and operating active distribution grids," *IET Generation, Transmission & Distribution*, vol. 11, no. 3, pp. 685–695, 2017.

[12] P. Fortenbacher, A. Ulbig, S. Koch, and G. Andersson, "Grid-constrained optimal predictive power dispatch in large multi-level power systems with renewable energy sources, and storage devices," in *IEEE PES Innovative Smart Grid Technologies, Europe*, Oct. 2014, pp. 1–6.

[13] VDE-AR-N 4105, "Power generation systems connected to the LV distribution network." FNN, Tech. Rep., 2011.

[14] E. Vrettos and G. Andersson, "Scheduling and Provision of Secondary Frequency Reserves by Aggregations of Commercial Buildings," *IEEE Transactions on Sustainable Energy*, vol. 7, no. 2, pp. 850–864, 4 2016.

[15] K. Strunz, E. Abbasi, C. Abbey, C. Andrieu, F. Gao, T. Gaunt, A. Gole, N. Hatziargyriou, and R. Iravani, "Benchmark Systems for Network Integration of Renewable and Distributed Energy Resources," *CIGRE, Task Force C6.04*, no. 273, pp. 4–6, 4 2014.